

# Robust Extrinsic Symmetry Estimation in 3D Point Clouds

Rajendra Nagar<sup>1\*</sup>

<sup>1\*</sup>Department of Electrical Engineering, Indian Institute of Technology Jodhpur,  
Jodhpur, 342037, Rajasthan, India, rn@iitj.ac.in.

Corresponding author(s). E-mail(s): [rn@iitj.ac.in](mailto:rn@iitj.ac.in);

## Abstract

Detecting the reflection symmetry plane of an object represented by a 3D point cloud is a fundamental problem in 3D computer vision and geometry processing due to its various applications, such as compression, object detection, robotic grasping, 3D surface reconstruction, etc. There exist several efficient approaches for solving this problem for clean 3D point clouds. However, it is a challenging problem to solve in the presence of outliers and missing parts. The existing methods try to overcome this challenge mostly by voting-based techniques but do not work efficiently. In this work, we proposed a statistical estimator-based approach for the plane of reflection symmetry that is robust to outliers and missing parts. We pose the problem of finding the optimal estimator for the reflection symmetry as an optimization problem on a 2-Sphere that quickly converges to the global solution for an approximate initialization. We further adapt the heat kernel signature for symmetry invariant matching of mirror symmetric points. This approach helps us to decouple the chicken-and-egg problem of finding the optimal symmetry plane and correspondences between the reflective symmetric points. The proposed approach achieves comparable mean ground-truth error and 4.5% increment in the F-score as compared to the state-of-the-art approaches on the benchmark dataset.

**Keywords:** Reflection Symmetry, Point Clouds, Statistical Estimation, Optimization, Heat Kernel Signatures

## 1 Introduction

Real-world objects exhibit various kinds of symmetry. For example, architectural sites and houses exhibit reflection and translation symmetry, and human-made objects, such as vehicles, household objects, and furniture, exhibit rotational and reflection symmetry. Apart from human-made objects, most living objects, such as humans, animals, and insects, also exhibit reflection symmetry. The role of symmetry present in objects is to make objects physically balanced for smooth navigation and make objects visually attractive.

The fundamental problems in computer vision, computer graphics, and geometry processing mainly focus on processing and analyzing objects

such as object detection and classification, physics-based photo-realistic rendering of objects, and 3D shape matching and texture transfer. Efficiently solving these problems requires a feature-level understanding of objects. The symmetry of objects plays a critical role in solving these problems [35, 43, 65, 74] and many other application problems such as reconstructing 3D model of face from a single image [71], estimating 3D pose [20], image matching and recognition [18], face expression classification [44], reconstructing 3D models of objects from a single image [28, 41, 64], spectral shape correspondences and texture transfer [40, 51], 3D registration [23], 3D Shape Completion [1, 61] and image re-colorization [36].

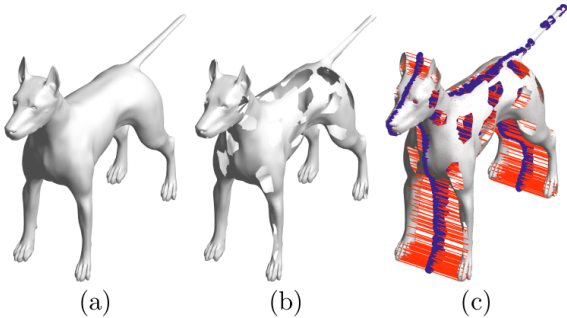


**Fig. 1** (a) Reflection symmetry of complete objects can be found efficiently [15]. However, the 3D point cloud of an object can be partial due to occlusions as shown in (b). Detecting symmetries from partial point clouds is a challenging and an open problem. In this work, we propose a statistical estimation-based algorithm for efficiently detecting symmetry of partial objects as shown in (c).

Symmetry is classified into three fundamental categories: reflection, rotation, and translation. Also, depending on the amount of occlusion and noise present while acquiring a digital representation of an object, we can classify the symmetry as approximate or exact symmetry, partial or complete symmetry, and single or multiple symmetries. Also, the symmetry can be classified further as extrinsic symmetry (rigid objects such as a building) or intrinsic symmetry (dynamic objects such as animals and humans) based on the distance preserved (Euclidean or geodesic distance, respectively) under self-isometry transformation. An object can be represented in many formats, such as digital images, 3D point clouds, triangle meshes, implicit surfaces, etc. The problem of detecting various types of symmetries in different forms of object representations has been an active problem of research in the vision and graphics communities [15, 35, 43].

In this work, we propose an algorithm to find the global reflection symmetry plane of an object represented as a 3D point cloud acquired through a 3D scanner. We solve this problem in the presence of noisy points and missing parts of the objects. In literature, many efficient algorithms exist for detecting exact and complete symmetry of objects represented as 3D point clouds [15]. However, detecting approximate and partial symmetry is an open problem [15] and lacks a generalized formulation for detecting this form of symmetry. Most of the existing methods follow voting-based strategies for handling outliers and

missing parts but fail to detect symmetry in the presence of a large number of outlier points and large missing parts [32, 42, 57]. Also, these methods construct a symmetry affinity matrix between the points that become intractable for large point clouds.

The state-of-the-art approaches [8, 12, 46] pose the problem of detecting the plane of symmetry as an optimization problem. They use the L2-norm as a metric to find the residuals and assume that the set of correspondences between the reflective symmetric points does not contain many outliers correspondences. However, in practice, the set of correspondences between the mirror reflective points may contain many outliers correspondences due to sensor noise, missing parts, and non-ideal feature descriptors. Also, the approaches proposed in [8, 12, 46] used iterative closest point (ICP) based approaches where the plane of symmetry and correspondences between symmetric points are found simultaneously using an iterative algorithm. Since the L2-norm is not robust to outliers, the efficiency of these methods degrades in challenging settings. In this work, we propose a statistical estimator for the plane of reflection symmetry that is robust to outliers and missing parts efficiently. The idea is to use  $L_2E$  estimator proposed in [3] that has been used ([24, 37, 38, 62]) to solve many other problems in computer vision and computer graphics. The penalty curve for the L2 norm is quadratic and assigns high probabilities even for outliers. Hence, its performance is affected by the outliers. Whereas the  $L_2E$  estimator assigns very low probabilities for many of the residuals that help it be efficient in the presence of outliers. We further decouple the problem of finding the correspondences and the plane of symmetry to make the proposed approach computationally efficient. We first estimate a set of putative correspondences between mirror symmetric points. We then propose an approach to find reflection symmetry invariant descriptors for points. We use the heat diffusion characteristics (Heat Kernel Signature [60]) for finding descriptors for points. Since the heat diffusion process is an intrinsic property of the shape which is invariant to rigid self-isometry [48], the proposed HKS-based descriptor, we name it Sym-HKS, is reflection symmetry invariant. Then, we pose the problem of finding an estimator for the plane of

reflection symmetry and its distance from the origin as an optimization problem on a unit 2-Sphere. We show that the proposed approach achieves state-of-the-art performance on the benchmark dataset [15]. In Figure 1, we show an example result.

**Contributions:** Our main contributions are the following.

1. An HKS-based 3D point descriptor that is invariant to reflection symmetry transformation and a symmetry-aware matching method for finding mirror symmetric correspondences.
2. Statistical estimators for the reflection symmetry plane and its distance from the origin, which are robust to a significant number of outliers and missing parts due to occlusions.
3. We formulate the problem of finding the estimator as an optimization problem on 2-Sphere and then solve it using an optimization on manifolds technique.

The remaining sections of the papers are organized as follows. In Section 2, we report the relevant research available in the literature and their limitations towards solving the symmetry detection problem efficiently. In Section 3, we describe the proposed algorithm for detecting reflection symmetry. In Section 3.2, we define a manifold optimization problem for finding an estimator for the plane of reflection symmetry that is robust to outliers and missing parts. In Section 4, we describe each point of the point cloud using a proposed descriptor that is reflection symmetry invariant descriptor. In Section 5, we describe the evaluation procedure and the evaluation for measuring the performance of the proposed approach on the benchmark dataset.

## 2 Related Work

The extrinsic reflection symmetry detection problem in 3D objects represented by triangle meshes and 3D point clouds is a hot topic of research in the computer vision and graphics and 3D geometry processing community due to its various algorithmic advantages in terms of computational complexity, geometric representation, and applications [14, 43]. In computer graphics and geometry processing literature, there exist many automatic algorithms for detecting the plane of reflection symmetry.

The approach proposed in Zabrodsky *et al.* [74] detect the reflection symmetry plane in a 2D point set. However, it needs a set of correct correspondences between mirror symmetric points computed in advance. The approaches proposed by Lipman *et al.* [32] and Xu *et al.* [72] find mirror-symmetric points using surface normals. They follow a voting-based approach and find symmetry orbits but need to tune various hyper-parameter. Also, for the approach proposed in [32], finding the symmetry factored embedding matrix becomes computationally intractable for larger size point clouds. Nagar and Raman used an optimization-based approach to find the plane of reflection symmetry in 3D point clouds with the provable guarantee of convergence of their method with a proper initialization [46]. However, this approach requires solving an integer linear program that becomes computationally intractable for large point clouds and does not detect partial symmetry. The method proposed in [30] uses multiple viewpoints of a 3D model to detect the plane of reflection symmetry. Whereas our approach can detect symmetry using only one viewpoint. The algorithm proposed by Combés *et al.* [10] detects reflection symmetry in a given 3D point cloud with a mild presence of outliers. This approach requires many hyper-parameters to be tuned, and it is computationally intractable as it requires solving an expectation maximization based problem at multiple scales.

The symmetry detection algorithms proposed by Mitra *et al.* [42], Speciale *et al.* [59], and Shi *et al.* [57] use point features to find reflection symmetry on 3D point clouds. These approaches use a voting-based approach to find the reflection symmetry plane that depends on the proper parameterization of the transformed space and require proper detection of modes in the transformed domain. Also, these approaches require a large number of pairs of points for voting that become intractable for large point clouds. Method proposed by Martinet *et al.* [39] uses moment functions to detect symmetry and the method proposed by Berner *et al.* [5] finds reflection symmetry using a graph constructed based on slippage features. However, these require graph connectivity for the input point clouds. The method proposed by Cohen *et al.* [9] uses the image features of pixels to find reflection symmetry in the structure from motion framework. However, it depends on image

features to find symmetry efficiently. Cicconet *et al.* [8] proposed a 3D registration based-approach. They first reflect the input point cloud about a random symmetry plane and then register both the point clouds to find the reflection symmetry plane. Ecins *et al.* proposed a symmetric model fitting-based algorithm that is not robust to missing parts [12]. Also, they require segmentation of the symmetric object to find the symmetry. These two algorithms [8] and [12] formulate the problem of symmetry estimation as a 3D rigid registration problem that increases the parameters of the reflection symmetry transformation as rotation matrix has three parameters for 3D registration, but the reflection symmetry plane has only two parameters to estimate. This leads an increased computational complexity. Hruda *et al.* proposed an efficient method where they proposed a differential measure for reflection symmetry in 3D point clouds [21, 22]. However, the performance of this method does not perform well for non-uniformly sampled point clouds. Also, it is robust to missing parts but may fail in presence of many scattered outlier points. Whereas, the proposed approach is robust to such cases.

There are various exciting approaches that use surface features to detect symmetry, such as [25, 29, 63]. However, these approaches can not directly be adapted to work on volumetric point clouds as the features used in these approaches assume that the point cloud is sampled from a 2-manifold surface. Ovsjanikov *et al.* [48], Qiao *et al.* [50] Wang *et al.* [67], Nagar and Raman [45], Xu *et al.* [73], Wang *et al.* [68], Liu *et al.* [33], Sahilliouglu *et al.* [53], and Sipiran *et al.* [58] use spectral properties of the Laplace-Beltrami operator and Kim *et al.* [26] use Möbius transformation to detect intrinsic symmetries of 3D objects represented by triangle meshes. However, these methods do not generalize to find extrinsic symmetry in 3D point clouds as they depend on mesh connectivity between points and assume that the underlying object is represented by a 2-manifold surface. The problem of reflection symmetry detection in digital images also is an active field of research [15, 17, 54, 56, 76]. However, these methods may not be generalized to detect 3D symmetry in point clouds due to completely different representations of objects. The problem of symmetry plane estimation and correspondences estimation is chicken-and-egg problem. In order

to solve this, we first have to find a set of correspondences between mirror symmetric points. Estimating correspondences between symmetric points is a challenging problem to solve [52, 66].

Recently, the problem of detecting reflection symmetry in 2D and 3D data has been addressed using learning based techniques. Shi *et al.* detect reflection as well as rotational symmetry in RGB-D data [56]. Zhou *et al.* learn a neural detector for detecting 3D symmetry of an object from a single RGB image [76]. Seo *et al.* use polar matching convolution for detecting 2D symmetries in an RGB image [54]. The current state-of-the-art method by Gao *et al.* uses neural networks for detecting 3D symmetries in point cloud data [16].

## 3 Proposed Approach

### 3.1 Problem Formulation

Let  $\mathcal{P} = \{\mathbf{x}_i\}_{i=1}^n \subset \mathbb{R}^3$  be a noisy and incomplete point cloud sampled from the surface of a symmetric object. Let  $\mathbf{v} \in \mathbb{R}^3$  be a unit norm vector that is normal to the plane of reflection symmetry and  $\omega$  be the distance of the symmetry plane from the origin. We can mathematically model the reflection symmetry using the Householder transform. That is, if  $\mathbf{x}$  and  $\mathbf{y}$  are reflective symmetric points, then  $\mathbf{y} = (\mathbf{I} - 2\mathbf{v}\mathbf{v}^\top)\mathbf{x} + 2\omega\mathbf{v}$ . Given the point cloud  $\mathcal{P}$ , we pose the problem of estimating  $\omega$  and  $\mathbf{v}$  as the below optimization problem.

$$\arg \min_{\substack{\omega \in \mathbb{R}, \mathbf{v} \in \mathbb{R}^3 \\ \mathbf{v}^\top \mathbf{v} = 1}} \sum_{i=1}^n \|\mathbf{x}_{\pi(i)} - (\mathbf{I} - 2\mathbf{v}\mathbf{v}^\top)\mathbf{x}_i - 2\omega\mathbf{v}\|_2^2. \quad (1)$$

Here,  $\mathbf{x}_{\pi(i)}$  denotes the reflection of the point  $\mathbf{x}_i$  about the symmetry plane. We can easily find the optimal  $\omega$  that minimizes this optimization problem by setting the derivative of the cost function which is defined as  $\omega = \frac{1}{n} \sum_{i=1}^n \mathbf{v}^\top (\frac{\mathbf{x}_i + \mathbf{x}_{\pi(i)}}{2})$ . Now, we replace this optimal  $\omega$  back in the optimization function and we rewrite the above formulation by observing that  $\|\mathbf{x}_{\pi(i)} - (\mathbf{I} - 2\mathbf{v}\mathbf{v}^\top)\mathbf{x}_i - 2\omega\mathbf{v}\|_2^2 = 4\mathbf{v}^\top \mathbf{x}_i \mathbf{x}_{\pi(i)}^\top \mathbf{v} + \|\mathbf{x}_i - \mathbf{x}_{\pi(i)}\|_2^2 - 4\omega\mathbf{v}^\top (\mathbf{x}_{\pi(i)} + \mathbf{x}_i) + 4\omega^2$ . Therefore, the optimization problem defined in Equation (1) for solving for  $\mathbf{v}$  is equivalent to the problem defined in

Equation (2).

$$\mathbf{v}^* = \arg \min_{\mathbf{v} \in \mathbb{R}^3, \mathbf{v}^\top \mathbf{v} = 1} \mathbf{v}^\top \mathbf{H} \mathbf{v}. \quad (2)$$

Here, the matrix  $\mathbf{H} \in \mathbb{R}^{3 \times 3}$  is defined as  $\mathbf{H} = \sum_{i=1}^n \mathbf{x}_i \mathbf{x}_{\pi(i)}^\top$ . A closed form solution to this problem can easily be found by minimizing the function  $\mathbf{v}^\top \mathbf{H} \mathbf{v} + \lambda(\mathbf{v}^\top \mathbf{v} - 1)$ . The optimal vector  $\mathbf{v}^*$  that minimizes this function is the eigenvector of the matrix  $\mathbf{H}$  corresponding to the smallest eigenvalue. In order to find the matrix  $\mathbf{H}$ , we should know the reflection point  $\mathbf{x}_{\pi(i)}$  for each point  $\mathbf{x}_i$ . However, we can not find the point of reflection without knowing the plane of reflection symmetry. Therefore, we have to solve two coupled problems: Find the symmetry plane  $(\mathbf{v}, \omega)$  using the mirror symmetric correspondences  $\{(\mathbf{x}_i, \mathbf{x}_{\pi(i)})\}_{i=1}^n$  and find the mirror symmetric correspondences  $\{(\mathbf{x}_i, \mathbf{x}_{\pi(i)})\}_{i=1}^n$  using the plane of reflection symmetry  $(\mathbf{v}, \omega)$ . Here, both  $(\mathbf{v}, \omega)$  and  $\{(\mathbf{x}_i, \mathbf{x}_{\pi(i)})\}_{i=1}^n$  are unknown. Hence, the problem defined in Equation (2) requires both correspondences as well as the plane of reflection symmetry which depend on each other. We know that given the correspondences between the mirror symmetric points, finding the optimal  $(\mathbf{v}, \omega)$  is easy as it is the eigenvector corresponding to the smallest eigenvalue of the matrix  $\mathbf{H}$ . However, finding correspondences  $(\mathbf{x}_i, \mathbf{x}_{\pi(i)})$  amounts to solving a linear assignment problem. This can become intractable for large point clouds. In order to solve this problem efficiently, we make use of surface features. In Section 4, we propose an approach to find symmetry aware feature descriptors for the input point cloud.

### 3.2 Robust Symmetry Plane Estimation

The set of putative correspondences we get through matching the reflection invariant feature descriptors may contain many outlier correspondences. The reason for this is that there can be many outlier points present in the given point cloud. Also, some parts of the object may be missing, that leads to wrong matches for points whose mirror reflective points are missing. The optimal symmetry plane  $(\mathbf{v}, \omega)$ , found by solving the optimization problem defined in Equation (2), as L2-norm is not robust to outliers.

In order to find the optimal symmetry plane  $(\mathbf{v}, \omega)$ , we propose a statistical estimation technique based on the  $L_2E$  estimator. Let  $\{(\mathbf{x}_i, \mathbf{x}_{\pi(i)})\}_{i=1}^n$  be a set of correspondences between mirror-symmetric points that may contain outlier correspondences. Now, we model the estimation problem as follows:

$$\mathbf{x}_{\pi(i)} = (\mathbf{I} - 2\mathbf{v}\mathbf{v}^\top)\mathbf{x}_i + 2\omega\mathbf{v} + \boldsymbol{\epsilon}, \quad i \in \{1, \dots, n\}. \quad (3)$$

Here,  $\boldsymbol{\epsilon} \in \mathbb{R}^3$  is noise and we assume that it follows the Gaussian distribution with zero mean and  $\sigma^2$  variance. I.e.,  $\boldsymbol{\epsilon} \sim \mathcal{N}(\mathbf{0}, \text{diag}([\sigma^2 \ \sigma^2 \ \sigma^2]))$  and all its samples are identically and independently distributed. Let us assume that the true symmetry plane parameters are  $(\mathbf{v}_0, \omega_0)$ . Now, let  $g(\mathbf{r} \mid \mathbf{v}, \omega)$  be the parametric density model with respect to the estimation parameters  $\mathbf{v}$  and  $\omega$ . Let  $g(\mathbf{r} \mid \mathbf{v}_0, \omega_0)$  be the parametric density model with respect to the true parameters  $\mathbf{v}_0$  and  $\omega_0$ . Here,  $\mathbf{r}$  denotes the residual vector. Then, the  $L_2E$  estimator  $\hat{\mathbf{v}}$  for  $\mathbf{v}_0$  and  $\hat{\omega}$  for  $\omega_0$  are found by minimizing the loss  $\int (g(\mathbf{r} \mid \mathbf{v}, \omega) - g(\mathbf{r} \mid \mathbf{v}_0, \omega_0))^2 d\mathbf{r}$  with respect to  $\mathbf{v}$  and  $\omega$ . Following the theory of L2E [3], the optimal  $\hat{\mathbf{v}}$  and  $\hat{\omega}$  can be found by solving the optimization problem defined in Equation (4) with respect to  $\mathbf{v}$  and  $\omega$ .

$$\min_{\substack{\omega \in \mathbb{R}, \mathbf{v} \in \mathbb{R}^3 \\ \mathbf{v}^\top \mathbf{v} = 1}} \int g^2(\mathbf{r} \mid \mathbf{v}, \omega) d\mathbf{r} - \frac{2}{n} \sum_{i=1}^n g(\mathbf{r}_i \mid \mathbf{v}, \omega). \quad (4)$$

Since we assume that the  $\boldsymbol{\epsilon}$  is the white Gaussian noise the residual vectors  $\mathbf{r}_i = \mathbf{x}_{\pi(i)} - (\mathbf{I} - 2\mathbf{v}\mathbf{v}^\top)\mathbf{x}_i - 2\omega\mathbf{v}$  follow a Gaussian distribution,

$$\text{i.e., } g(\mathbf{r}_i \mid \mathbf{v}, \omega) = \frac{1}{(2\pi\sigma^2)^{\frac{3}{2}}} e^{-\frac{\|\mathbf{x}_{\pi(i)} - (\mathbf{I} - 2\mathbf{v}\mathbf{v}^\top)\mathbf{x}_i - 2\omega\mathbf{v}\|_2^2}{2\sigma^2}}.$$

Also, since  $g(\mathbf{r} \mid \mathbf{v}, \omega)$  is a Gaussian distribution the term  $\int g^2(\mathbf{r} \mid \mathbf{v}, \omega) d\mathbf{r} = \frac{1}{(2\pi\sigma^2)^{\frac{3}{2}}}$  which is constant with respect to the parameters  $\mathbf{v}$  and  $\omega$ . Hence, the  $L_2E$  estimators  $\hat{\mathbf{v}}$  and  $\hat{\omega}$  for  $\mathbf{v}$  and  $\omega$ , respectively, can be defined as in Equation (5).

$$\begin{aligned} &= \max_{\substack{\omega \in \mathbb{R}, \mathbf{v} \in \mathbb{R}^3 \\ \mathbf{v}^\top \mathbf{v} = 1}} \sum_{i=1}^n \frac{2}{n(2\pi\sigma^2)^{\frac{3}{2}}} e^{-\frac{\|\mathbf{x}_{\pi(i)} - (\mathbf{I} - 2\mathbf{v}\mathbf{v}^\top)\mathbf{x}_i - 2\omega\mathbf{v}\|_2^2}{2\sigma^2}} \\ &= \max_{\substack{\omega \in \mathbb{R}, \mathbf{v} \in \mathbb{R}^3 \\ \mathbf{v}^\top \mathbf{v} = 1}} f(\mathbf{v}, \omega). \end{aligned} \quad (5)$$



Now, in order to find the optimal estimators  $(\hat{\mathbf{v}}, \hat{\omega})$  for  $(\mathbf{v}, \omega)$ , we have to find the maximum of the function  $f$  with respect to  $\mathbf{v}$  and  $\omega$ . We follow an *alternating optimization* approach to find the optimal parameters. We first initialize  $\mathbf{v}$  (which we describe at the end of this section) and find optimal  $\omega$ . Then, we update  $\mathbf{v}$  with the new  $\omega$ . We keep alternating between these two optimization problems till convergence. We first describe the approach for finding optimal  $\mathbf{v}$  given  $\omega$ .

**Optimal  $\mathbf{v}$ :** We observe that the domain of the function  $f$  is the 2-Sphere  $\mathbb{S}^2 = \{\mathbf{v} \in \mathbb{R}^3 \mid \mathbf{v}^\top \mathbf{v} = 1\}$ , which is a smooth 2-manifold [2]. Therefore, in order to solve the problem defined in Equation (5) with respect to  $\mathbf{v}$ , we use the technique of optimization on manifolds [2]. We find the Riemannian gradient of the function  $f$  on the manifold  $\mathbb{S}^2$  by first finding the Euclidean gradient on the tangent plane and then projecting it to the sphere as follows. Let  $\nabla f(\mathbf{v})$  be the Euclidean gradients and  $\text{grad}f(\mathbf{v})$  be the Riemannian gradient of the function  $f$ . Then, the Riemannian and the Euclidean gradients are related as  $\text{grad}f(\mathbf{v}) = \mathbb{P}_{\mathbf{v}}(\nabla f(\mathbf{v}))$ . Here,  $\mathbb{P}_{\mathbf{v}}$  is the projection operator for  $\mathbb{S}^2$  that projects an ambient space vector onto the tangent space at  $\mathbf{v}$  and defined as  $\mathbb{P}_{\mathbf{v}}(\mathbf{x}) = \mathbf{x} - (\mathbf{x}^\top \mathbf{v})\mathbf{v}$ . The Euclidean gradient of the function  $f(\mathbf{v}, \omega) = \frac{2}{n(2\pi\sigma^2)^{\frac{3}{2}}} \sum_{i=1}^n e^{-\frac{f_i(\mathbf{v}, \omega)}{2\sigma^2}}$  can easily be found by and is defined in Equation (6). Here,  $f_i(\mathbf{v}, \omega) = 4\mathbf{v}^\top \mathbf{C}_i \mathbf{v} + \|\mathbf{x}_i - \mathbf{x}_{\pi(i)}\|_2^2 - 4\omega \mathbf{v}^\top (\mathbf{x}_{\pi(i)} + \mathbf{x}_i) + 4\omega^2$ .

$$\begin{aligned} \nabla f(\mathbf{v}) &= \sum_{i=1}^n \frac{8\omega \mathbf{m}_i - 4(\mathbf{C}_i + \mathbf{C}_i^\top) \mathbf{v}}{n\sigma^2(2\pi\sigma^2)^{\frac{3}{2}}} e^{-\frac{f_i(\mathbf{v}, \omega)}{2\sigma^2}} \\ &= \frac{4(\mathbf{1}_n^\top \otimes \mathbf{I}_3)[(\mathbf{A} \odot (\omega \mathbf{D} - \mathbf{B}(\mathbf{I} \otimes \mathbf{v}))]\mathbf{1}_n}{n\sigma^2(2\pi\sigma^2)^{\frac{3}{2}}}. \end{aligned} \quad (6)$$

Here,  $\mathbf{m}_i = \frac{\mathbf{x}_{\pi(i)} + \mathbf{x}_i}{2}$ ,  $\mathbf{C}_i = \mathbf{x}_i \mathbf{x}_{\pi(i)}^\top$ ,  $\mathbf{A} \in \mathbb{R}^{3n \times 3n}$  is a block diagonal matrix where the  $i$ -th diagonal block is defined as  $e^{-\frac{f_i(\mathbf{v}, \omega)}{2\sigma^2}} \mathbf{I}_3$ , the matrix  $\mathbf{B} \in \mathbb{R}^{3n \times 3n}$  is also a diagonal matrix where the  $i$ -th diagonal block is equal to  $\mathbf{C}_i + \mathbf{C}_i^\top$ , the matrix  $\mathbf{D} \in \mathbb{R}^{3n \times 3n}$  is a diagonal matrix where the  $i$ -th diagonal block is equal to  $\mathbf{x}_i + \mathbf{x}_{\pi(i)}$ ,  $\mathbf{I}$  is the identity matrix of size  $n \times n$ ,  $\mathbf{1}_n \in \{1\}^n$ ,  $\otimes$  is the Kronecker matrix product operator, and  $\odot$  is the

element-wise matrix multiplication operator. We use the Manifold-BFGS optimization algorithm, proposed in [2], for finding the optimal solution. We use the *manopt* toolbox for optimization on manifolds [6].

We further observe that the function  $f$  is not a convex function and is locally convex around the global maximum. Therefore, the final solution and the convergence rate depend on the initialization of vector  $\mathbf{v}$ .

**Optimal  $\omega$ :** Given the initialized  $\mathbf{v}$ , the function  $f(\mathbf{v}, \omega)$  is a non-convex function with respect to  $\omega$ . Therefore, we solve this non-linear and non-convex optimization problem using the BFGS (Broyden–Fletcher–Goldfarb–Shanno) Quasi-Newton algorithm [13]. We provide the exact and explicit derivative of the cost function  $\frac{\partial f(\mathbf{v}, \omega)}{\partial \omega}$  to make the BFGS optimization algorithm to converge faster, which is defined in Equation (7).

$$\frac{\partial f(\mathbf{v}, \omega)}{\partial \omega} = \frac{4}{n} \sum_{i=1}^n \frac{\mathbf{v}^\top (\mathbf{x}_{\pi(i)} + \mathbf{x}_i) - 2\omega}{\sigma^2(2\pi\sigma^2)^{\frac{3}{2}}} e^{-\frac{f_i(\mathbf{v}, \omega)}{2\sigma^2}}. \quad (7)$$

**Initialization of  $\mathbf{v}$ :** The normal vector to the symmetry plane is perpendicular to the plane containing the mid-points of the to the vectors joining mirror symmetric points (i.e.,  $(\mathbf{x}_i)$  and  $\mathbf{x}_{\pi(i)}$ ). Therefore, in case of clean and complete point clouds, we may initialize the vector  $\mathbf{v}$  as the eigenvector of the matrix  $\frac{1}{n} \sum_{i=1}^n \left( \frac{\mathbf{x}_i + \mathbf{x}_{\pi(i)}}{2} \right) \left( \frac{\mathbf{x}_i + \mathbf{x}_{\pi(i)}}{2} \right)^\top$  corresponding to the smallest eigenvalue. This is the classical principle component analysis approach. However, in case of noisy correspondences, the classical PCA may fail to find the initial  $\mathbf{v}$  approximately. We, therefore, use the Grassmann manifold averaging based robust PCA algorithm [19]. We use the Robust Grassmann Average (RGA) algorithm to find the vectors  $\eta_1$  and  $\eta_2$  that spans the subspace represented by the set of mid-points  $\left\{ \frac{\mathbf{x}_i + \mathbf{x}_{\pi(i)}}{2} \right\}_{i=1}^n$  of the line segments joining the mirror-symmetric points  $\mathbf{x}_i$  and  $\mathbf{x}_{\pi(i)}$ . Then, we initialize  $\mathbf{v} = \eta_1 \times \eta_2$ .

**A Remark on MLE:** We would like to clarify that the cost function, defined in Equation (5), for the L2E estimator is different than the maximum likelihood estimator (MLE). We can easily determine the MLE estimator  $\mathbf{v}_{\text{mle}}$  as by solving the

below optimization problem:

$$\begin{aligned} \mathbf{v}_{\text{mle}} &= \arg \max_{\mathbf{v} \in \mathbb{R}^3, \mathbf{v}^\top \mathbf{v}^\top = 1} \frac{1}{(2\pi\sigma^2)^{\frac{3n}{2}}} e^{-\frac{2}{\sigma^2} \sum_{i=1}^n \mathbf{v}^\top \mathbf{x}_i \mathbf{x}_{\pi(i)}^\top \mathbf{v}} \\ \mathbf{v}_{\text{mle}} &= \arg \min_{\mathbf{v} \in \mathbb{R}^3, \mathbf{v}^\top \mathbf{v}^\top = 1} \sum_{i=1}^n \mathbf{v}^\top \mathbf{x}_i \mathbf{x}_{\pi(i)}^\top \mathbf{v}. \end{aligned} \quad (8)$$

We can observe that the cost functions of  $L_2E$  estimator and MLE estimators defined in Equation (8), respectively, are different. In Section 4.1, we analyse the robustness of the  $L_2E$  and the MLE estimators in presence of outliers.

## 4 Mirror Symmetric Point Correspondences

Our goal is to find a set of candidate matching between mirror symmetric points to find the plane of reflective symmetry plane. Since the proposed algorithm for finding the normal vector to the plane of reflection symmetry is robust to outlier matches, our aim is to find a set with a few correct correspondences where other correspondences can be outliers. In order to find a set  $\{(\mathbf{x}_i, \mathbf{x}_{\pi(i)})\}_{i=1}^n$  of putative correspondences between the mirror-symmetric points, we need to find the mapping  $\pi : \{1, 2, \dots, n\} \rightarrow \{1, 2, \dots, n\}$ . In order to find the matching  $\pi$ , we first find a set of feature points and their symmetry invariant descriptors and then solve a matching problem.

**Sym-HKS: Feature Point Detection and Description.** In order to find the mirror symmetric feature points, we use the Intrinsic Shape Signature (ISS) approach proposed by Zhong 2009 [75] as the feature points detected by this approach are intrinsic. Therefore, it detects intrinsically symmetric points on the given point cloud. Let  $\{\mathbf{o}_i\}_{i=1}^a$  be the set of detected  $a$  ISS keypoints. Now, we find a feature descriptor for each of the detected ISS keypoint using the heat kernel signatures technique Sun et al. 2009 [60]. There exist other approaches for feature description (such as [31, 69, 70]). However, we prefer HKS over the other approaches as it is reflection symmetry and scale invariant. The HKS requires the eigenfunctions of the Laplace Beltrami operator. Therefore, we first construct the Laplacian Beltrami operator of the surface defined by the input point cloud using the approach proposed by Sharp and Crane

2020 [55]. There exist other approaches (such as [4],[34]) for finding the LBO for point clouds, but they mostly work for manifold surfaces and not scale for non-manifold surfaces such as a chair. Most of the objects in practice have non-manifold surfaces. The Tufted Laplacian algorithm proposed in [55] finds the Laplacian matrix and the vertex area matrix for the surface defined by the input points with requiring the points connectivity. We solve the generalized eigenvalue problem  $\mathbf{L}\phi_i = \lambda_i \mathbf{M}\phi_i$  to find the eigenfunctions corresponding to the first  $k$  smallest eigenvalues of the Laplace Beltrami operator. Here  $\mathbf{L}$  is the sparse Laplacian matrix and  $\mathbf{M}$  is the diagonal mass matrix. Now, the heat kernel signature  $\mathbf{h}_i \in \mathbb{R}^p$  of the  $i$ -th ISS keypoint  $\mathbf{o}_i$  is defined in Equation (9)

$$\mathbf{h}_i = \left[ \sum_{j=1}^k e^{-t_0 \lambda_j} \phi_j^2(\mathbf{o}_i) \dots \sum_{j=1}^k e^{-t_{p-1} \lambda_j} \phi_j^2(\mathbf{o}_i) \right]^\top. \quad (9)$$

Here,  $t_0, \dots, t_{p-1}$  are  $p$  time instances uniformly spaced in the range  $\left[ \frac{10 \log_e(10)}{\lambda_k}, \frac{10 \log_e(10)}{\lambda_2} \right]$  as suggested in [60].

**Estimating Mirror Symmetric Correspondences.** In order to find a set of putative correspondences between mirror symmetric points, we can use the HKSs of the feature points as the HKS for mirror symmetric points would be the same. In order to find the mirror symmetric point of the keypoint  $\mathbf{o}_i$ , we can find the keypoint from the set  $\{\mathbf{o}_i\}_{i=1}^a \setminus \{\mathbf{o}_i\}$  which has the closest HKS with that of the  $\mathbf{o}_i$ . However, this strategy may fail in general due to the following reason. Let us consider three points  $\mathbf{o}_i, \mathbf{o}_j$ , and  $\mathbf{o}_\ell$  such that  $\mathbf{o}_j$  is a neighbor of  $\mathbf{o}_i$  and  $\mathbf{o}_\ell$  is the mirror reflection of  $\mathbf{o}_i$ . Now, since  $\mathbf{o}_i$  and  $\mathbf{o}_j$  are neighbors and the eigenfunctions are at least twice differentiable (as they are the solution of the Laplace equation) hence  $\phi(\mathbf{o}_i) \approx \phi(\mathbf{o}_j)$ . Therefore, the HKS  $\mathbf{h}_i$  and  $\mathbf{h}_j$  would be similar as  $\|\mathbf{h}_i - \mathbf{h}_j\|_2^2 = \sum_{g=0}^{p-1} (\sum_{i=1}^k e^{-t_g \lambda_i} (\phi_i^2(\mathbf{o}_i) - \phi_i^2(\mathbf{o}_j)))^2 \approx 0$ . This may result in multiple neighbor matches  $(\mathbf{o}_i, \mathbf{o}_j)$ . Therefore, we must ensure that the nearby points are not matched. To enforce this constraint, we need a way of measuring the closeness of the points on the surface defined by the point cloud. Geodesic distance is one of the best options, but it would require connectivity of the points and may be computationally inefficient for large point

clouds.

We circumvent this challenge by using the eigenfunctions of the Laplace Beltrami operator as follows which we have already computed to find HKS. Let  $\mathbf{s}_i = [s_{i0} \ s_{i1} \ \dots \ s_{ia}]$  be the sign vector for the feature point  $\mathbf{o}_i$  where  $s_{ij} = +1$  if  $\phi_j(\mathbf{o}_i) \geq 0$  and  $s_{ij} = -1$  if  $\phi_j(\mathbf{o}_i) < 0$ . Now, if the two points are neighbors, they would be in the same nodal set of low-frequency eigenfunctions. Therefore,  $\mathbf{s}_i = \mathbf{s}_j$  for the two neighboring points  $\mathbf{o}_i$  and  $\mathbf{o}_j$ . However, if we consider two mirror symmetric points  $\mathbf{o}_i$  and  $\mathbf{o}_\ell$  which lie on the two different halves of the objects, then they would lie on different nodal domains which might have different signs as some of the eigenfunctions of the Laplace Beltrami operator would be having negative signs (equivalent to odd functions in the Euclidean sense). Therefore,  $\|\mathbf{s}_i - \mathbf{s}_\ell\|_2$  will be very high for the two mirror symmetric points. With this approach, we formulate the following optimization approach, which prohibits neighboring points matchings and ensures mirror symmetric points matching.

$$\max_{\mathbf{P} \in \{0,1\}^{k \times k}} \sum_{i=1}^k \sum_{j=1}^k p_{ij} a_{ij} \quad (10)$$

$$\text{subject to } \mathbf{1}^\top \mathbf{P} \leq \mathbf{1}^\top \quad (11)$$

$$\mathbf{P} \mathbf{1} \leq \mathbf{1} \quad (12)$$

$$\mathbf{1}^\top \mathbf{P} \mathbf{1} = 2q \quad (13)$$

Here,  $a_{ij} = \|\mathbf{h}_i - \mathbf{h}_j\|_2 + \psi(\|\mathbf{s}_i - \mathbf{s}_j\|_2)$ ,  $\psi(t) = b$  if  $t = 0$  and  $\phi(t) = 0$  for  $t > 0$ . Here,  $b$  is a very large constant which we set equal to 1000 in our experiment. The matrix  $\mathbf{P} \in \{0,1\}^{k \times k}$  is the binary matching matrix with its  $(i,j)$ -th entry defined as  $p_{ij} = 1$  if the feature points  $\mathbf{o}_i$  and  $\mathbf{o}_j$  form are mirror symmetric images of each other and  $p_{ij} = 0$ , otherwise. The constant  $q$  denotes the number of mirror symmetric correspondences we want, which would ensure that we choose the best  $q$  candidate correspondences. This optimization problem is a standard linear integer program that we solve using the `intlinprog` function in the MATLAB.

## 4.1 Complete Algorithm and Analysis

Now, we present the complete method for finding the normal vector to the plane of reflection

---

### Algorithm 1 Robust Reflection Symmetry Plane Estimation

---

**Input:** A 3D Point cloud  $\mathcal{P} = \{\mathbf{x}_i\}_{i=1}^n$

- 1:  $\mathbf{L} \leftarrow \text{Tufted-LB0}(\mathcal{P}) \triangleright \text{find LBO Eigenfunctions}$
- 2:  $\{(\mathbf{x}_i, \mathbf{x}_{\pi(i)})\}_{i=1}^n \leftarrow \text{Sym-HKS}(\mathbf{L}) \triangleright \text{correspondences}$
- 3:  $\mathbf{O} \leftarrow \left[ \frac{\mathbf{x}_1 + \mathbf{x}_{\pi(1)}}{2} \ \dots \ \frac{\mathbf{x}_n + \mathbf{x}_{\pi(n)}}{2} \right]^\top$
- 4:  $\mathbf{v} \leftarrow \text{RGA}(\mathbf{O}) \triangleright \text{find initial } \mathbf{v}$
- 5:  $\mathbf{C}_i \leftarrow \mathbf{x}_{\pi(i)} \mathbf{x}_i^\top, \forall i \{1, 2, \dots, n\}$ .
- 6:  $\mathbf{B} \leftarrow \text{diag} \left( [\mathbf{C}_1 + \mathbf{C}_1^\top \ \dots \ \mathbf{C}_n + \mathbf{C}_n^\top] \right)$
- 7:  $\mathbf{D} \leftarrow \text{diag} \left( [(\mathbf{x}_1 + \mathbf{x}_{\pi(1)}) \ \dots \ (\mathbf{x}_n + \mathbf{x}_{\pi(n)})] \right)$
- 8: **while** not converged **do**  $\triangleright$  Alternating optimization
- 9:      $\omega \leftarrow \text{BFGS}(f(\mathbf{v}, \omega), \frac{\partial f(\mathbf{v})}{\partial \omega}) \triangleright \text{find } \omega \text{ given } \mathbf{v}$
- 10:     **while** not converged **do**  $\triangleright \text{find } \mathbf{v} \text{ given } \omega$
- 11:          $\mathbf{A} \leftarrow \text{diag} \left( \left[ e^{-\frac{f_1(\mathbf{v}, \omega)}{2\sigma^2}} \mathbf{1}_3 \ \dots \ e^{-\frac{f_n(\mathbf{v}, \omega)}{2\sigma^2}} \mathbf{1}_3 \right] \right)$
- 12:          $\beta \leftarrow \frac{4(\mathbf{1}_n^\top \otimes \mathbf{I}_3)[(\mathbf{A} \odot (\omega \mathbf{D} - \mathbf{B}(\mathbf{I} \otimes \mathbf{v}))]\mathbf{1}_n}{n\sigma^2(2\pi\sigma^2)^{\frac{3}{2}}}$
- 13:          $\text{grad}f(\mathbf{v}) \leftarrow \beta - \beta^\top \mathbf{v} \mathbf{v} \triangleright \text{Riemannian gradient}$
- 14:          $\mathbf{v} \leftarrow \text{Manifold-BFGS}(\text{grad}f(\mathbf{v}), f, \mathbf{v})$
- 15:     **end while**
- 16: **end while**

**Output:**  $\mathbf{v}, \omega$ .

---

symmetry given a 3D point cloud in Algorithm 1. In Figure 2, we demonstrate the robustness of our approach for outliers. In the first row, we add a different number of outlier correspondences (blue color lines) and perturb the ground-truth correspondences (orange color lines) between the symmetric mirror points. In the second row, we show the actual global minimum (green color point) of the cost function defined in Equation (1). We observe that if we directly optimize this cost function, the estimated solution (red color point) quickly moves away from the global solution as we increase the number of outlier correspondences. This is the main limitation of the state-of-the-art methods ([12],[8],[46],[47]) as they minimize the L2-norm based cost function. Whereas, we minimize the  $L_2E$  cost function  $-f$  defined in Equation (5) that can assign low probabilities to many outlier correspondences and hence the estimated solution (shown in 3rd row by blue color) remains close to the global solution even with a significant number of outliers. Here, we have shown the cost functions on 2-Sphere  $S^2$ . In Figure 3, we plot the deviation angle  $\theta$  between the estimated normal vector and the ground-truth normal vector for the proposed approach ( $\cos^{-1}(|$



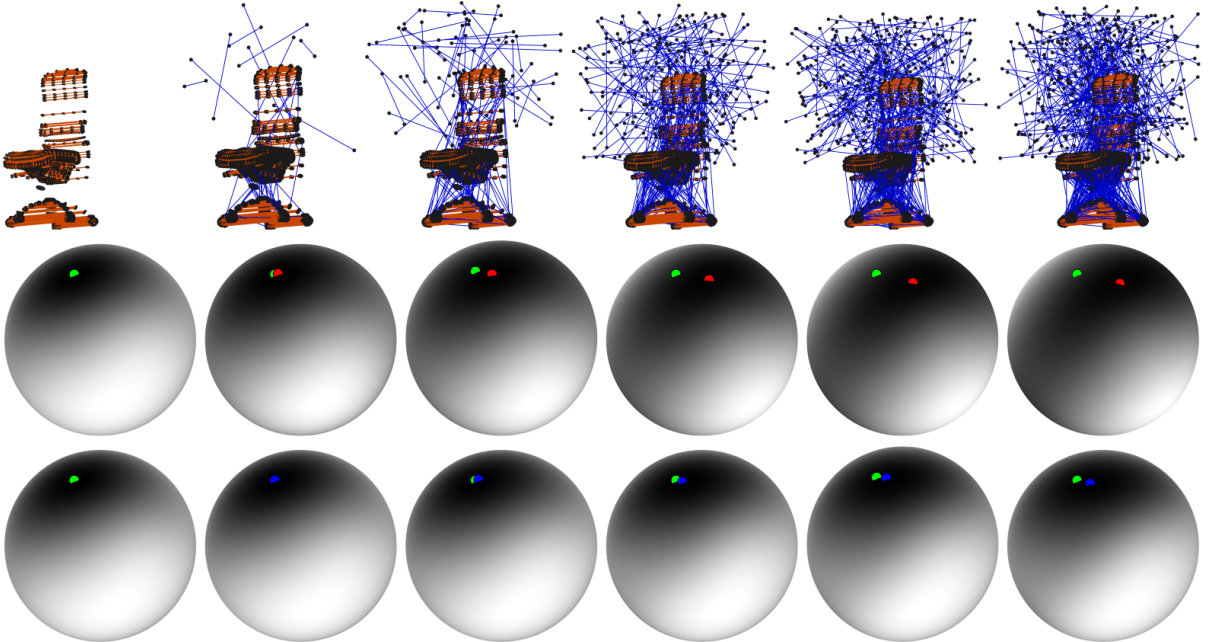


**Fig. 2** In 1st row, we increase outlier matches (blue lines) and perturb true matches (orange lines). In 2nd row, we show the true minimum (green point) of the function (MLE estimator) defined in Equation (8). The estimated solution (red point) obtained by minimizing it quickly moves away from the true solution as we increase outliers. This is the main limitation of existing methods ([12],[8],[46],[47]) as they use L2-norm based cost function. We minimize an  $L_2E$  estimator based cost function  $-f$  that assigns low probabilities to many outlier and hence the estimated solution (3rd row, blue points) remains nearby to the global solution even with many outliers. We show cost functions on  $\mathbb{S}^2$ .

$\mathbf{v}_g^\top \mathbf{v}_p$ )) and for the baseline method ( $\cos^{-1}(|\mathbf{v}_g^\top \mathbf{v}_b|)$ ). Here, the baseline approach is equivalent to solving the optimization problem proposed in Equation (2). We observe that the deviation for the proposed approach remains very small ( $< 7^\circ$ ) even for a large number of outlier correspondences (65%).

## 5 Results and Evaluation

### 5.1 Evaluation of Reflection Symmetry Plane

#### Benchmark Dataset and Evaluation Metric:

In order to test the performance of the proposed approach, we find the accuracy of detecting the symmetry plane. We use the benchmark dataset and the standard evaluation metric proposed by Funk *et al.* [15]. Funk *et al.* published a dataset of 1354 objects represented as 3D point clouds exhibiting single reflection symmetry. We compare the accuracy of detection of plane of symmetry with the accuracies that of the state-of-the-art methods proposed by Cicconet *et al.* [8], Ecins

*et al.* [12], Speciale *et al.* [59], Hruda [22], and Nagar and Raman [47]. We use the F-score as a performance measure metric proposed by Funk *et al.* [15]. We also compare the accuracy of symmetry detection with the accuracy that of the methods proposed by Cicconet *et al.* [8] and Nagar and Raman [47] for the detection of partial and approximate symmetry detection. We first find the precision and recall rates and then use them to find the F-score. The precision rate of detecting symmetry plane is defined as  $p_r = \frac{t_p}{t_p + f_p}$ , the recall rate of detection of symmetry plane is defined as  $r_c = \frac{t_p}{t_p + f_n}$ , and the value of the F-Score is defined as  $f_s = \frac{2p_r \times r_c}{p_r + r_c}$ . Here, we define the quantities  $t_p$  (true positives),  $f_p$  (false positives), and  $f_n$  (false negatives) as follows:  $t_p$  is the number of correctly detected planes of symmetry,  $f_p$  is the number of incorrectly detected planes of symmetry, and  $f_n$  is the number of undetected ground-truth planes of symmetry. In the benchmark dataset, the ground symmetry plane is defined by three points on it  $\mathbf{p}_a$ ,  $\mathbf{p}_b$ , and  $\mathbf{p}_c$ . Let us assume that the points  $\mathbf{q}_a$ ,  $\mathbf{q}_b$ , and  $\mathbf{q}_c$  be any

three non co-linear points on the estimated plane of symmetry. Then, according to Funk *et al.*, the detected plane of symmetry is correct if the angle between the normals of the ground-truth plane of symmetry  $\mathbf{g}_n = (\mathbf{p}_a - \mathbf{p}_b) \times (\mathbf{p}_a - \mathbf{p}_c)$  and the esti-

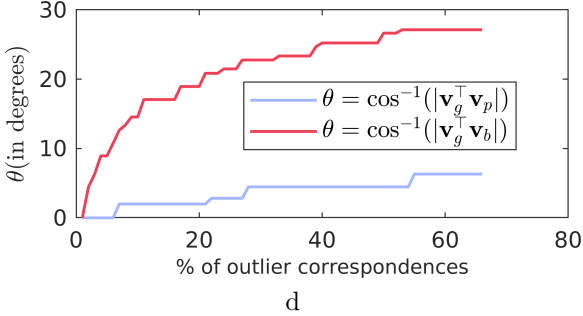


**Fig. 3** The deviation angle between the estimated and ground-truth normal vectors for the proposed approach ( $\cos^{-1}(|\mathbf{v}_g^T \mathbf{v}_p|)$ ) and for the baseline method ( $\cos^{-1}(|\mathbf{v}_g^T \mathbf{v}_b|)$ ).

imated plane of symmetry  $\mathbf{e}_n = (\mathbf{q}_a - \mathbf{q}_b) \times (\mathbf{q}_a - \mathbf{q}_c)$  is smaller than a predefined threshold. Also, the distance between the center of the ground-truth plane of symmetry  $\mathbf{g}_c = \frac{\mathbf{p}_a + \mathbf{p}_c}{2}$  and the center of the detected plane of reflection symmetry  $\mathbf{e}_c = \frac{\mathbf{q}_a + \mathbf{q}_c}{2}$  should be smaller than a given threshold  $t_d$  on the distance. We change the value of the threshold  $t_a$  on angle criterion in the range  $[0, \frac{\pi}{4}]$  and the value of the threshold  $t_d$  on the distance criterion in the range  $[0, 2s]$ . Here, the constant  $s$  is defined to be equal to  $\min\{\|\mathbf{p}_a - \mathbf{p}_b\|_2, \|\mathbf{p}_a - \mathbf{p}_c\|_2, \|\mathbf{q}_a - \mathbf{q}_b\|_2, \|\mathbf{q}_a - \mathbf{q}_c\|_2\}$ . Since this dataset contains perfectly symmetric objects with no outliers, we define the center of the plane of symmetry as the mean center of the input point cloud. Hence, the distance threshold criterion is true for all the approaches. In Figure 4, we plot the recall vs precision curves for the algorithms proposed by Cicconet *et al.* [8], Ecins *et al.* [12], Speciale *et al.* [59], Hruda [22], and Nagar and Raman [47]. We observe that the value of the F-score (0.93) for the proposed approach is the highest among all methods. The benchmark dataset [15] contains complete objects. Therefore the performance of the method proposed in [47] is comparable to the performance of the proposed approach. In Figure 5, we plot the estimated normal vectors to symmetry planes, a few sampled points (red

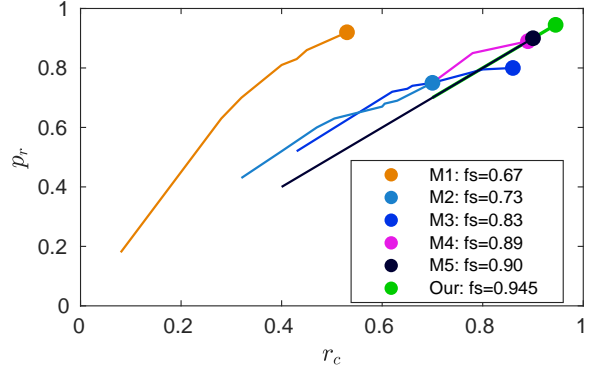


**Fig. 4** Precision ( $p_r$ ) vs Recall ( $r_c$ ) curve for the methods proposed by Cicconet *et al.* [8] (M1), Ecins *et al.* [12] (M2), Speciale *et al.* [59] (M3), Hruda [22] (M4), Nagar and Raman [47] (M5), and our method on the benchmark dataset [15].

color points) on the detected plane, and correspondences between mirror symmetric points (blue color lines) using the proposed approach for a few 3D point clouds from the dataset [11]. We observe that our method can detect symmetry of objects using their partial scans in the presence of outlier points. We have also used our algorithm on dynamic model (last model of second row of Figure 5). We observe that the proposed approach is able to detect the symmetry in the extrinsically symmetric parts (hands for the first model and legs for the second model). There are some mirror symmetric correspondences (as HKS is invariant to isometric deformations) detected in the non-symmetric region, but they are not accurate enough. Actually, the dynamic models exhibit intrinsic symmetry, and there is a separate category of algorithms for solving this problem, e.g. [26, 45, 48].

## 5.2 Evaluation of Partial Symmetry Detection

In order to measure the performance of our approach and compare it with the performances of the other state-of-the-art methods [47] and [22] on 3D objects with missing parts, we follow the same evaluation process proposed in Section 5.1 and the dataset proposed in [15]. This dataset has partial scans of 20 real-world objects along with their ground-truth plane of symmetry. The average value of the F-Score for the methods in [46], [22], and for proposed algorithm are 0.90, 0.93, and 0.96, respectively. We obtain higher



**Fig. 5** Results of the proposed approach on the eight models with significant missing parts from the dataset [11].

F-score for partial scan than that for the complete scans since the partial scan dataset contains only 20 models whereas the dataset for complete scans contains 1354 models. In Figure 6, we show detected planes for two model from this dataset.

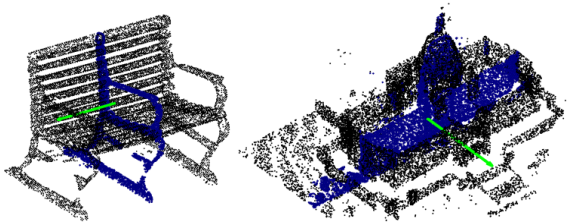


**Fig. 6** Results of the proposed approach on the two models from the partial and real scan dataset [15].

### 5.3 Symmetry Distance Error and Ground-Truth Error

We compare the performance of the proposed approach with a recent state-of-the-art learning based algorithm PRSNet [16] and classical algorithms [25], [39], [42], [49], and [27] on the ShapeNet dataset [7]. We follow the evaluation metrics symmetry distance error (SDE) and ground-truth error (GTE) as proposed in [16]. The SDE is defined as the distance between the original point cloud and the reflected point cloud using the detected symmetry plane. The GTE is defined as the euclidean distance between the distance between the ground truth symmetry plane and detected symmetry plane. In Table 1, we present

the SDE and the GTE for these approaches. We observe that the proposed approach has better performance than the classical approaches and comparable performance with that of the PRSNet algorithm (a supervised learning based approach) and Kazhdan et al. [25].

### 5.4 Effect of Outliers and Missing Parts

In order to measure the performance in presence of a significant amount of outliers, we use the strategy proposed in [47]. We again consider the 3D objects provided in dataset [15] and introduce random points into the input 3D point cloud to get a modified noisy point cloud  $\mathcal{P}^n = \mathcal{P} \cup \mathcal{P}_r$ . Here, the point cloud  $\mathcal{P}_r$  is a set of outliers. We choose different number of noise points such that  $|\mathcal{P}_r| = \frac{\alpha}{100} |\mathcal{P}|$ ,  $\alpha \in \{0, 20, \dots, 120\}$ . We find the value of the F-score for the method proposed in [47] and the proposed algorithm for every value of the new point cloud  $\mathcal{P}^n$ . We use the dataset [15] for evaluation. In Table 2 present the obtained F-score values for different values of  $\alpha$ . We observe that even for the case where half of the points are outliers, the F-score for the proposed approach remains around 0.88. To measure the performance of our method and compare it with that of the state-of-the-art methods for partial symmetry, we remove a set  $\mathcal{P}_m$  of connected points from the input 3D point cloud  $\mathcal{P}$  such that  $|\mathcal{P}_m| = \gamma |\mathcal{P}|$ ,  $\gamma \in \{0, 0.15, 0.20, 0.28\}$  and find the value of F-score for the method proposed in [47] and the proposed algorithm. We use the dataset [15] for evaluation. In Table 3, we present the obtained F-score values for different values of  $\gamma$ . We note that even for  $\gamma = 0.28$ , F-score for the proposed approach remains 0.89. In Figure 7, we show detected planes for a few models from the dataset [22] to show that the proposed approach is robust to noisy points. We present a qualitative result compared with [47] in Figure 8. The main reason for the failure of the method [47] is that the symmetry plane detection algorithm fails to converge to the final solution if the angle between the initialized normal vector and the ground-truth normal vector is more than around  $20^\circ$ . We observe that there are many outlier matches to a part (neck and chest) for which the mirror part does not exist. In the presence of many outliers and missing parts, this initialize

**Table 1** The mean ground truth error (GTE) and the mean symmetry distance error (SDE) of for the different methods on the 1000 models of different categories of the ShapeNet [7] dataset.

Error	PCA	Kazhdan [25]	Martinet [39]	Mitra [42]	PRST [49]	Korman [27]	PRS-Net [16]	RANSAC	Ours New
GTE( $\times 10^{-2}$ )	2.41	0.17	13.6	52.1	4.42	19.2	<b>0.11</b>	1.53	0.13
SDE( $\times 10^{-4}$ )	3.32	0.897	3.95	14.2	1.78	1.75	<b>0.86</b>	2.31	0.89

**Table 2** The value of F-score for the proposed approach and [47] as we vary the value of  $\alpha$  in  $\{0, 20, \dots, 100\}$ .

$\alpha \rightarrow$	0	20	40	60	80	100
[47]	0.90	0.87	0.86	0.86	0.85	0.85
Proposed	0.95	0.94	0.92	0.91	0.91	0.89

algorithm fails to properly initialize the normal vector. Whereas, the proposed estimator is significantly robust (angle error  $< 7\%$ ) to many outlier correspondences (65%) and produces good matches at the convergence.

**Table 3** The value of F-score for the proposed approach and [47] as we vary the value of  $\gamma$  in the range  $\{0, 0.15, 0.20, 0.28\}$ .

$\gamma \rightarrow$	0	0.15	0.20	0.28
[47]	0.90	0.82	0.75	0.67
Proposed	0.95	0.93	0.92	0.90

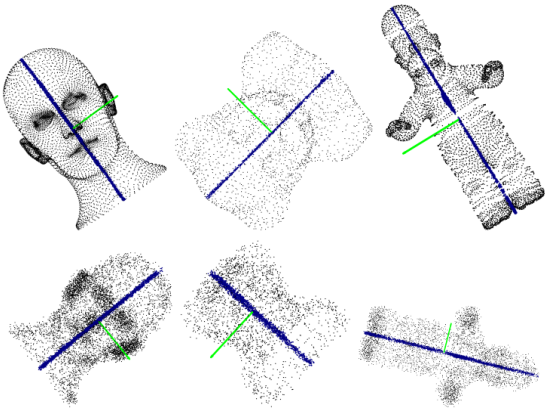


**Fig. 7** The first row represents the detected symmetries in clean models. The second row represents the detected symmetries in noisy models (models are from the work [22]).

## 5.5 Time Complexity:

The BFGS method takes  $\mathcal{O}(n)$  [2]. The descriptor finding step takes  $\mathcal{O}(nh^2)$ , ( $\mathcal{O}(h^2)$  for finding eigenvalues of  $\mathbf{D}$ ). Here,  $h$  is the average number of neighboring points. For our experiments

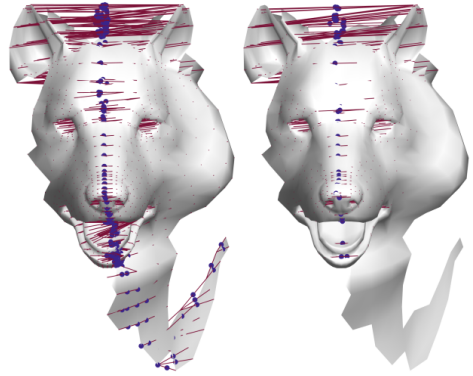


**Fig. 8** Left: Result of the approach proposed in [47] on a partial model. Right: Result of the proposed approach on the same partial model.

$h \approx 100$ . Therefore, the overall approximate time complexity of our approach is  $\mathcal{O}(n) + \mathcal{O}(nh^2)$ . The time complexity of the method proposed in [46] is  $\mathcal{O}(n^{3.5})$ . For a model with 5k points,  $k = 20$  and  $r = 0.1$ , our algorithm takes around 1.58 seconds on a Linux OS with an Intel-i7 processor. We report the time comparison in Table 4. We observe that the computation time for the method proposed in [47] increases drastically ( $\mathcal{O}(n \log n)$ ) for large point clouds as it solves a nearest-neighbor search problem for updating mirror correspondences in each iteration. Our algorithm finds a robust estimator for the symmetry plane even from noisy mirror correspondences and does not require solving the nearest-neighbor problem. We need to run Manifold-BFGS solver to find  $\mathbf{v}$  which has only two variables. Hence, our computational complexity is almost linear in point cloud size.

We have also compared the computation time

**Table 4** Computation time comparison with [47] on the dataset [15].

#Vertices	5k	10k	50k	100k	300k
[47]	0.38s	0.48s	6.12s	16.03s	61.01s
Proposed	2.15s	3.67s	5.23s	8.13s	12.92s

for the proposed approach with that of the methods proposed in Korman *et al.* [27], Mitra *et al.*



**Table 5** Computation time (in sec) for Korman *et al.* [27], Mitra *et al.* [42], Gao *et al.* [16], and proposed approach.

Method	[27]	[42]	[16]	Proposed
Time (s)	0.97	0.42	0.0018	0.21

[42], and Gao *et al.* [16]. We have used i7 processor for comparing the computation time. We have used 3D models having around 1042 vertices. In Table 5, we present the computation for these approaches. We observe that the proposed approach has the second best computation time. It is the best among non-learning based approaches. The method proposed in [16] achieves the best test computation time which is a learning based approached.

## 5.6 Missing Part Completion using the Detected Symmetry

In order to show the practical application of the proposed approach, we use the detected symmetry of partial symmetric objects to reconstruct the missing parts. Let  $\mathcal{P} = \{\mathbf{x}_i\}_{i=1}^n$  be an incomplete point cloud exhibiting reflection. Let  $\mathbf{v}$  be the estimated normal vector to the symmetry plane of the object represented by  $\mathcal{P}$ . Then, we reconstruct the complete object as  $\mathcal{P} \cup \mathcal{Q}$  where  $\mathcal{Q} = \{(\mathbf{I} - 2\mathbf{v}\mathbf{v}^\top)\mathbf{x}_i + 2\omega\mathbf{v}\}_{i=1}^n$ . In Figure 9, we show a few partial objects and the completed objects using this approach.

## 6 Conclusion

In this work, we have proposed a fast and robust algorithm for detecting symmetry of 3D objects exhibiting single reflection symmetry and represented by partial and noisy points clouds. We adapted a statistical estimation technique for finding the plane of reflection symmetry. For this purpose, we first found a 3D point descriptor for each point that is invariant to reflection symmetry transformation. Then, we used an approximate nearest neighbor matching technique for finding a set of candidate correspondences between mirror reflective points. We used this set of putative correspondences and a statistical estimator to estimate the reflection symmetry plane that is robust to a significant number of outliers and missing parts. The proposed approach achieved comparable mean ground-truth error and 4.5% increment

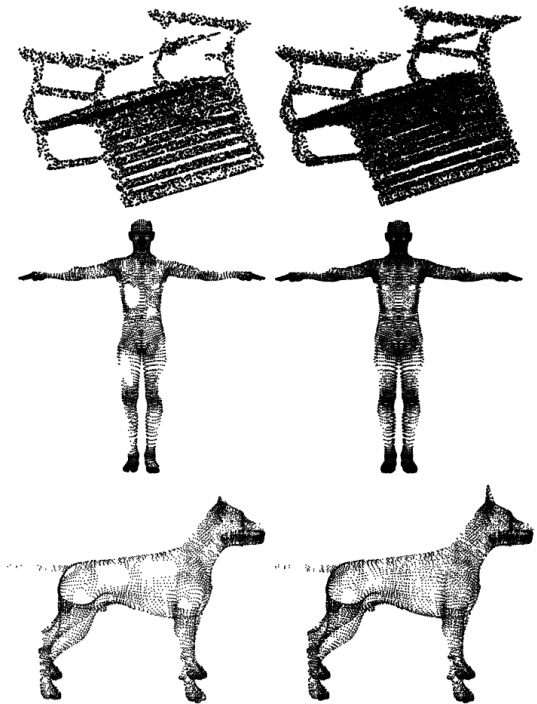


**Fig. 9** Object completion using the detected reflection symmetry. First Column: Incomplete Objects. Second Column: Symmetry Guided Completion.

in the F-score as compared to the state-of-the-art approaches on the benchmark dataset.

**Limitations and Future Works:** The proposed work only detects the global intrinsic reflection symmetry of a given 3D model represented by a point cloud. However, many objects may reflect local symmetry along with global symmetry, e.g. a building. In future work, we would like to extend our framework for detecting symmetries objects exhibiting multiple reflection symmetries. Furthermore, the proposed approach detects extrinsic reflection symmetry in a point cloud. We would further like to extend the proposed approach for detecting intrinsic symmetries of non-rigid objects.

**Acknowledgments:** This work was funded by the SERB, Government of India with through the Start-up Research Grant (SRG) scheme.

## References

- [1] Ali Abbasi, Sinan Kalkan, and Yusuf Sahillioğlu. Deep 3d semantic scene extrapolation. *The Visual Computer*, 35:271–279, 2019.



- [2] P-A Absil, Robert Mahony, and Rodolphe Sepulchre. *Optimization algorithms on matrix manifolds*. Princeton University Press, 2009.
- [3] Ayanendranath Basu, Ian R Harris, Nils L Hjort, and MC Jones. Robust and efficient estimation by minimising a density power divergence. *Biometrika*, 85(3):549–559, 1998.
- [4] Mikhail Belkin, Jian Sun, and Yusu Wang. Constructing laplace operator from point clouds in rd. In *Proceedings of the twentieth annual ACM-SIAM symposium on Discrete algorithms*, pages 1031–1040. SIAM, 2009.
- [5] Alexander Berner, Martin Bokeloh, Michael Wand, Andreas Schilling, and Hans-Peter Seidel. A graph-based approach to symmetry detection. In *Volume Graphics*, volume 40, pages 1–8, 2008.
- [6] Nicolas Boumal, Bamdev Mishra, P-A Absil, and Rodolphe Sepulchre. Manopt, a matlab toolbox for optimization on manifolds. *The Journal of Machine Learning Research*, 15(1):1455–1459, 2014.
- [7] Angel X Chang, Thomas Funkhouser, Leonidas Guibas, Pat Hanrahan, Qixing Huang, Zimo Li, Silvio Savarese, Manolis Savva, Shuran Song, Hao Su, et al. Shapenet: An information-rich 3d model repository. *arXiv preprint arXiv:1512.03012*, 2015.
- [8] Marcelo Cicconet, David GC Hildebrand, and Hunter Elliott. Finding mirror symmetry via registration and optimal symmetric pairwise assignment of curves: Algorithm and results. In *IEEE International Conference on Computer Vision Workshop (ICCVW)*, pages 1759–1763. IEEE, 2017.
- [9] Andrea Cohen, Christopher Zach, Sudipta N Sinha, and Marc Pollefeys. Discovering and exploiting 3d symmetries in structure from motion. In *Computer Vision and Pattern Recognition (CVPR), 2012 IEEE Conference on*, pages 1514–1521. IEEE, 2012.
- [10] Benoît Combès, Robin Hennessy, John Waddington, Neil Roberts, and Sylvain Prima. Automatic symmetry plane estimation of bilateral objects in point clouds. In *Computer Vision and Pattern Recognition, 2008. CVPR 2008. IEEE Conference on*, pages 1–8. IEEE, 2008.
- [11] Luca Cosmo, Emanuele Rodolà, Michael M Bronstein, Andrea Torsello, Daniel Cremers, and Y Sahillioglu. Shrec’16: Partial matching of deformable shapes. *Proc. 3DOR*, 2(9):12, 2016.
- [12] Aleksandrs Eciņs, Cornelia Fermuller, and Yiannis Aloimonos. Detecting reflectional symmetries in 3d data through symmetrical fitting. In *Proceedings of the IEEE International Conference on Computer Vision Workshops*, pages 1779–1783, 2017.
- [13] Roger Fletcher. *Practical methods of optimization*. John Wiley & Sons, 2000.
- [14] Chris Funk and Yanxi Liu. Symmetry recaptcha. In *Proceedings of the IEEE Conference on Computer Vision and Pattern Recognition*, pages 5165–5174, 2016.
- [15] Christopher Funk, Seungkyu Lee, Martin R Oswald, Stavros Tsogkas, Wei Shen, Andrea Cohen, Sven Dickinson, and Yanxi Liu. 2017 iccv challenge: Detecting symmetry in the wild. In *Proceedings of the IEEE International Conference on Computer Vision Workshops*, pages 1692–1701, 2017.
- [16] Lin Gao, Ling-Xiao Zhang, Hsien-Yu Meng, Yi-Hui Ren, Yu-Kun Lai, and Leif Kobbelt. Prs-net: Planar reflective symmetry detection net for 3d models. *IEEE Transactions on Visualization and Computer Graphics*, 27(6):3007–3018, 2020.
- [17] Alessandro Gnutti, Fabrizio Guerrini, and Riccardo Leonardi. Combining appearance and gradient information for image symmetry detection. *IEEE Transactions on Image Processing*, 30:5708–5723, 2021.
- [18] Daniel Cabrini Hauagge and Noah Snavely. Image matching using local symmetry features. In *Computer Vision and Pattern Recognition (CVPR), 2012 IEEE Conference*

- on, pages 206–213. IEEE, 2012.
- [19] Soren Hauberg, Aasa Feragen, and Michael J Black. Grassmann averages for scalable robust pca. In *Proceedings of the IEEE Conference on Computer Vision and Pattern Recognition*, pages 3810–3817, 2014.
- [20] Tomas Hodan, Daniel Barath, and Jiri Matas. Epos: estimating 6d pose of objects with symmetries. In *Proceedings of the IEEE/CVF conference on computer vision and pattern recognition*, pages 11703–11712, 2020.
- [21] Lukáš Hruďa, Ivana Kolingerová, and Miroslav Lávička. Plane space representation in context of mode-based symmetry plane detection. In *International Conference on Computational Science*, pages 509–523. Springer, 2020.
- [22] Lukáš Hruďa, Ivana Kolingerová, and Libor Váša. Robust, fast and flexible symmetry plane detection based on differentiable symmetry measure. *The Visual Computer*, pages 1–17, 2021.
- [23] Lan Hu and Laurent Kneip. Globally optimal point set registration by joint symmetry plane fitting. *Journal of Mathematical Imaging and Vision*, pages 1–19, 2021.
- [24] Bing Jian and Baba C Vemuri. Robust point set registration using gaussian mixture models. *IEEE transactions on pattern analysis and machine intelligence*, 33(8):1633–1645, 2010.
- [25] Michael Kazhdan, Bernard Chazelle, David Dobkin, Adam Finkelstein, and Thomas Funkhouser. A reflective symmetry descriptor. In *European Conference on Computer Vision*, pages 642–656. Springer, 2002.
- [26] Vladimir G Kim, Yaron Lipman, Xiaobai Chen, and Thomas Funkhouser. Möbius transformations for global intrinsic symmetry analysis. In *Computer Graphics Forum*, volume 29, pages 1689–1700. Wiley Online Library, 2010.
- [27] Simon Korman, Roe'e Litman, Shai Avidan, and Alex Bronstein. Probably approximately symmetric: Fast rigid symmetry detection with global guarantees. In *Computer Graphics Forum*, volume 34, pages 2–13. Wiley Online Library, 2015.
- [28] Kevin Köser, Christopher Zach, and Marc Pollefeys. Dense 3d reconstruction of symmetric scenes from a single image. In *Pattern Recognition*, pages 266–275. Springer, 2011.
- [29] Ruxandra Lasowski, Art Tevs, Hans-Peter Seidel, and Michael Wand. A probabilistic framework for partial intrinsic symmetries in geometric data. In *Computer Vision, 2009 IEEE 12th International Conference on*, pages 963–970. IEEE, 2009.
- [30] Bo Li, Henry Johan, Yuxiang Ye, and Yijuan Lu. Efficient 3d reflection symmetry detection: A view-based approach. *Graphical Models*, 83:2–14, 2016.
- [31] Qinsong Li, Ling Hu, Shengjun Liu, Dangfu Yang, and Xinru Liu. Anisotropic spectral manifold wavelet descriptor. In *Computer Graphics Forum*, volume 40, pages 81–96. Wiley Online Library, 2021.
- [32] Yaron Lipman, Xiaobai Chen, Ingrid Daubechies, and Thomas Funkhouser. Symmetry factored embedding and distance. In *ACM Transactions on Graphics (TOG)*, volume 29, page 103. ACM, 2010.
- [33] Tianqiang Liu, Vladimir G Kim, and Thomas Funkhouser. Finding surface correspondences using symmetry axis curves. In *Computer Graphics Forum*, volume 31, pages 1607–1616. Wiley Online Library, 2012.
- [34] Yang Liu, Balakrishnan Prabhakaran, and Xiaohu Guo. Point-based manifold harmonics. *IEEE Transactions on visualization and computer graphics*, 18(10):1693–1703, 2012.
- [35] Yanxi Liu, Hagit Hel-Or, Craig S Kaplan, and Luc Van Gool. Computational symmetry in computer vision and computer graphics. *Foundations and Trends in Computer Graphics and Vision*, 5(1-2):1–195, 2010.

- [36] Michal Lukáč, Daniel Sýkora, Kalyan Sunkavalli, Eli Shechtman, Ondřej Jamriška, Nathan Carr, and Tomáš Pajdla. Nautilus: Recovering regional symmetry transformations for image editing. *ACM Transactions on Graphics*, 36(4), 2017.
- [37] Jiayi Ma, Ji Zhao, Jinwen Tian, Zhuowen Tu, and Alan L Yuille. Robust estimation of nonrigid transformation for point set registration. In *Proceedings of the IEEE conference on computer vision and pattern recognition*, pages 2147–2154, 2013.
- [38] M Mancas, B Gosselin, and B Macq. Fast and automatic tumoral area localisation using symmetry. In *Proceedings.(ICASSP'05). IEEE International Conference on Acoustics, Speech, and Signal Processing, 2005.*, volume 2, pages 725–728. IEEE, 2005.
- [39] Aurélien Martinet, Cyril Soler, Nicolas Holzschuch, and François X Sillion. Accurate detection of symmetries in 3d shapes. *ACM Transactions on Graphics (TOG)*, 25(2):439–464, 2006.
- [40] Simone Melzi, Jing Ren, Emanuele Rodolà, Abhishek Sharma, Peter Wonka, and Maks Ovsjanikov. Zoomout: spectral upsampling for efficient shape correspondence. *ACM Transactions on Graphics (TOG)*, 38(6):1–14, 2019.
- [41] Adersh Miglani, Sumantra Dutta Roy, Santanu Chaudhury, and JB Srivastava. Symmetry based 3d reconstruction of repeated cylinders. In *2013 Fourth National Conference on Computer Vision, Pattern Recognition, Image Processing and Graphics (NCVPRIPG)*, pages 1–4. IEEE, 2013.
- [42] Niloy J Mitra, Leonidas J Guibas, and Mark Pauly. Partial and approximate symmetry detection for 3d geometry. In *ACM Transactions on Graphics (TOG)*, volume 25, pages 560–568. ACM, 2006.
- [43] Niloy J Mitra, Mark Pauly, Michael Wand, and Duygu Ceylan. Symmetry in 3d geometry: Extraction and applications. In *Computer Graphics Forum*, volume 32, pages 1–23. Wiley Online Library, 2013.
- [44] Sinjini Mitra and Yanxi Liu. Local facial asymmetry for expression classification. In *Computer Vision and Pattern Recognition, 2004. CVPR 2004. Proceedings of the 2004 IEEE Computer Society Conference on*, volume 2, pages II–889. IEEE, 2004.
- [45] Rajendra Nagar and Shanmuganathan Raman. Fast and accurate intrinsic symmetry detection. In *Proceedings of the European Conference on Computer Vision (ECCV)*, pages 417–434, 2018.
- [46] Rajendra Nagar and Shanmuganathan Raman. Detecting approximate reflection symmetry in a point set using optimization on manifold. *IEEE Transactions on Signal Processing*, 67(6):1582–1595, 2019.
- [47] Rajendra Nagar and Shanmuganathan Raman. 3dsymm: robust and accurate 3d reflection symmetry detection. *Pattern Recognition*, 107:107483, 2020.
- [48] Maks Ovsjanikov, Jian Sun, and Leonidas Guibas. Global intrinsic symmetries of shapes. In *Computer graphics forum*, volume 27, pages 1341–1348. Wiley Online Library, 2008.
- [49] Joshua Podolak, Philip Shilane, Aleksey Golovinskiy, Szymon Rusinkiewicz, and Thomas Funkhouser. A planar-reflective symmetry transform for 3d shapes. *ACM Transactions on Graphics (TOG)*, 25(3):549–559, 2006.
- [50] Yi-Ling Qiao, Lin Gao, Shu-Zhi Liu, Ligang Liu, Yu-Kun Lai, and Xilin Chen. Learning-based real-time detection of intrinsic reflectional symmetry. *arXiv preprint arXiv:1911.00189*, 2019.
- [51] Jing Ren, Simone Melzi, Maks Ovsjanikov, and Peter Wonka. Maptree: recovering multiple solutions in the space of maps. *ACM Transactions on Graphics (TOG)*, 39(6):1–17, 2020.

- [52] Yusuf Sahilliođlu. Recent advances in shape correspondence. *The Visual Computer*, 36(8):1705–1721, 2020.
- [53] Yusuf Sahilliođlu and Yücel Yemez. Coarse-to-fine isometric shape correspondence by tracking symmetric flips. In *Computer Graphics Forum*, volume 32, pages 177–189. Wiley Online Library, 2013.
- [54] Ahyun Seo, Woohyeon Shim, and Minsu Cho. Learning to discover reflection symmetry via polar matching convolution. In *Proceedings of the IEEE/CVF International Conference on Computer Vision*, pages 1285–1294, 2021.
- [55] Nicholas Sharp and Keenan Crane. A laplacian for nonmanifold triangle meshes. In *Computer Graphics Forum*, volume 39, pages 69–80. Wiley Online Library, 2020.
- [56] Yifei Shi, Junwen Huang, Hongjia Zhang, Xin Xu, Szymon Rusinkiewicz, and Kai Xu. Symmetrynet: learning to predict reflectional and rotational symmetries of 3d shapes from single-view rgb-d images. *ACM Transactions on Graphics (TOG)*, 39(6):1–14, 2020.
- [57] Zeyun Shi, Pierre Alliez, Mathieu Desbrun, Hujun Bao, and Jin Huang. Symmetry and orbit detection via lie-algebra voting. In *Computer Graphics Forum*, volume 35, pages 217–227. Wiley Online Library, 2016.
- [58] Ivan Sipiran, Robert Gregor, and Tobias Schreck. Approximate symmetry detection in partial 3d meshes. In *Computer Graphics Forum*, volume 33, pages 131–140. Wiley Online Library, 2014.
- [59] Pablo Speciale, Martin R Oswald, Andrea Cohen, and Marc Pollefeys. A symmetry prior for convex variational 3d reconstruction. In *European Conference on Computer Vision*, pages 313–328. Springer, 2016.
- [60] Jian Sun, Maks Ovsjanikov, and Leonidas Guibas. A concise and provably informative multi-scale signature based on heat diffusion. In *Computer graphics forum*, volume 28, pages 1383–1392. Wiley Online Library, 2009.
- [61] Minhyuk Sung, Vladimir G Kim, Roland Angst, and Leonidas Guibas. Data-driven structural priors for shape completion. *ACM Transactions on Graphics (TOG)*, 34(6):1–11, 2015.
- [62] Vincent YF Tan and Cédric Févotte. Automatic relevance determination in nonnegative matrix factorization with the/spl beta/-divergence. *IEEE Transactions on Pattern Analysis and Machine Intelligence*, 35(7):1592–1605, 2012.
- [63] Dilip Mathew Thomas and Vijay Natarajan. Multiscale symmetry detection in scalar fields by clustering contours. *IEEE transactions on visualization and computer graphics*, 20(12):2427–2436, 2014.
- [64] Sebastian Thrun and Ben Wegbreit. Shape from symmetry. In *Computer Vision, 2005. ICCV 2005. Tenth IEEE International Conference on*, volume 2, pages 1824–1831. IEEE, 2005.
- [65] Christopher W Tyler. *Human symmetry perception and its computational analysis*. Psychology Press, 2003.
- [66] Oliver Van Kaick, Hao Zhang, Ghassan Hamarneh, and Daniel Cohen-Or. A survey on shape correspondence. In *Computer graphics forum*, volume 30, pages 1681–1707. Wiley Online Library, 2011.
- [67] Hui Wang and Hui Huang. Group representation of global intrinsic symmetries. In *Computer Graphics Forum*, volume 36, pages 51–61. Wiley Online Library, 2017.
- [68] Wencheng Wang, Junhui Ma, Panpan Xu, and Yiyao Chu. Intrinsic symmetry detection on 3d models with skeleton-guided combination of extrinsic symmetries. In *Computer Graphics Forum*, volume 38, pages 617–628. Wiley Online Library, 2019.
- [69] Yiqun Wang, Jianwei Guo, Dong-Ming Yan, Kai Wang, and Xiaopeng Zhang. A robust local spectral descriptor for matching non-rigid shapes with incompatible shape structures. In *Proceedings of the IEEE/CVF*

*Conference on Computer Vision and Pattern Recognition*, pages 6231–6240, 2019.

- [70] Yiqun Wang, Jing Ren, Dong-Ming Yan, Jianwei Guo, Xiaopeng Zhang, and Peter Wonka. Mgen: Descriptor learning using multiscale gcons. *ACM Transactions on Graphics (TOG)*, 39(4):122–1, 2020.
- [71] Shangzhe Wu, Christian Rupprecht, and Andrea Vedaldi. Unsupervised learning of probably symmetric deformable 3d objects from images in the wild. In *Proceedings of the IEEE/CVF Conference on Computer Vision and Pattern Recognition*, pages 1–10, 2020.
- [72] Kai Xu, Hao Zhang, Wei Jiang, Ramsay Dyer, Zhiqian Cheng, Ligang Liu, and Baoquan Chen. Multi-scale partial intrinsic symmetry detection. *ACM Transactions on Graphics (TOG)*, 31(6):181, 2012.
- [73] Kai Xu, Hao Zhang, Andrea Tagliasacchi, Ligang Liu, Guo Li, Min Meng, and Yueshan Xiong. Partial intrinsic reflectional symmetry of 3d shapes. In *ACM SIGGRAPH Asia 2009 papers*, pages 1–10. 2009.
- [74] Hagit Zabrodsky, Shmuel Peleg, and David Avnir. Symmetry as a continuous feature. *IEEE Transactions on Pattern Analysis and Machine Intelligence*, 17(12):1154–1166, 1995.
- [75] Yu Zhong. Intrinsic shape signatures: A shape descriptor for 3d object recognition. In *2009 IEEE 12th international conference on computer vision workshops, ICCV workshops*, pages 689–696. IEEE, 2009.
- [76] Yichao Zhou, Shichen Liu, and Yi Ma. Nerd: neural 3d reflection symmetry detector. In *Proceedings of the IEEE/CVF Conference on Computer Vision and Pattern Recognition*, pages 15940–15949, 2021.